Effect of neighboring topography on seismic motion in the sediment valley

Jozef Kristek, Peter Moczo and Erik Bystrický
Geophysical Institute, Slovak Academy of Sciences[1]

Abstract: A new P-SV hybrid modeling technique is used to investigate an effect that a neighboring topography may have on seismic motion in a sediment valley. Our example shows a considerable effect of a ridge on the horizontal component of seismic motion in the valley. This indicates that the neighboring topography should be taken into account even when we are only interested in the valley response.

Key words: hybrid modeling, finite-difference method, finite-element method, site effect

1. Introduction

The effects of local near-surface sedimentary structures (e.g., sediment-filled valleys and basins) and free-surface topographies (e.g., ridges and hills) on a seismic ground motion were investigated in numerous studies in two-three last decades. In most of those studies either sedimentary or topographic structures were investigated separately, see, for example, papers [1–4] for reviews and comprehensive lists of articles on site effects. It is well known, however, that many sedimentary basins and valleys are at least partly surrounded by mountain ranges. This fact inspired us to perform simple numerical modeling of the P-SV seismic motion in a sediment valley neighboring a ridge.

2. Models and method

We need to compute responses of the two local geologic structures - the sediment valley neighboring the ridge and the valley alone (i.e., without any neighboring topographic feature) due to the localized source, see Fig. 1a and b. A recently developed hybrid method [5] can be used for such a compu-

[1] Dúbravská cesta 9, 842 28 Bratislava, Slovakia

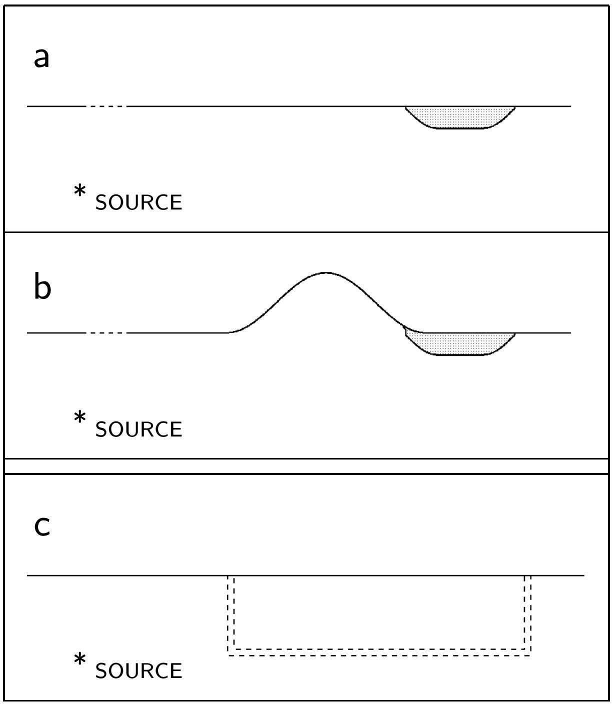

Fig. 1. Two models of the local structures. a: sediment valley, b: combined topographic-sedimentary structure. c: The source radiation and wave propagation in the background medium (i.e., homogeneous halfspace) is computed only once. The wavefield recorded along the excitation lines (dashed lines) is then used in response computation for each of the structures.

tation with advantage. This is because we can avoid computing the source radiation and background propagation twice (i.e., for each of the two models) by making use of the coupling algorithm. First, we compute the source radiation and background wave propagation in the absence of both irregularities (i.e., in the homogeneous halfspace) and record the wavefield along two excitation lines, see Fig. 1c. Second, we apply the recorded wavefield on the excitation lines in the computation for each of the two structures without including the physical localized source.

The other advantageous feature of our computations is a combined $2h \times 2h$ and $h \times h$ spatial grid (h being a grid spacing). While we perform the finite-difference computations on the $h \times h$ grid inside the excitation rectangle, we use the $2h \times 2h$ grid in a major part of the computational region. The link between the $h \times h$ and $2h \times 2h$ grids is accomplished using

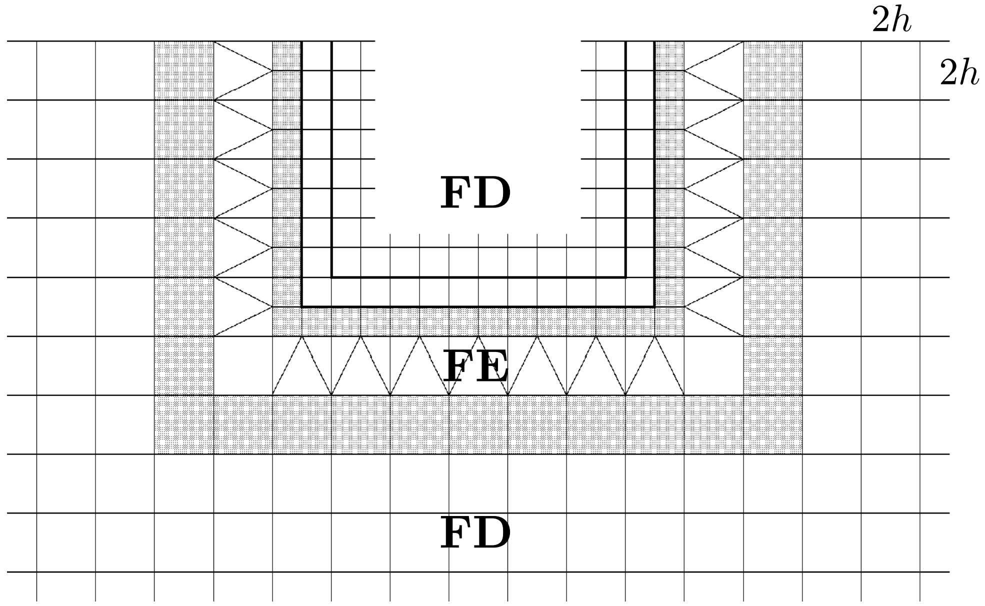

Fig. 2. The combined $h \times h$ and $2h \times 2h$ spatial grid. The finite elements (FE) are used as a transition zone between the two finite-difference (FD) grids.

a strip of finite elements - see Fig. 2. The combined grid significantly reduces the computer memory requirements.

In the numerical computations we considered the following model and source parameters: The topographic feature is a symmetric ridge having a cosine shape. The base of the ridge is 500 m wide and its elevation is 150 m. The shape of the valley is described by the function

$$f(x) = \begin{cases} -D\cos\left(\dfrac{\pi}{2}+\dfrac{x}{2}\right); & 0 \le x \le D\dfrac{\pi}{2} \\ D; & D\dfrac{\pi}{2} < x < W - D\dfrac{\pi}{2} \\ D\cos\left(\dfrac{\pi}{2}+\dfrac{x-W-D\pi}{D}\right); & W - D\dfrac{\pi}{2} \le x \le W. \end{cases}$$

Here D is the valley depth and W is the total valley width on the free surface. Our valley is 53 m deep and 275 m wide on the free surface. The P- and S- wave velocities, and the density inside the valley are 900 m/s, 400 m/s, and 1900 kg/m^3, respectively. The P- and S- wave quality factors are 60 and 40. The P- and S-wave velocities outside the valley are 2000 m/s and 1000 m/s, respectively. The P- and S-wave quality factors are 100 and 80. The quality factors are specified at the frequency of 6 Hz and the Futterman $Q(\omega)$ law is assumed. The $Q(\omega)$ law is approximated using three relaxation mechanisms. The wavefield is due to the downward vertical force acting along the line source that is in 300 m depth and 1010 m to the left of the left valley margin. The time step is 0.0005 s. The receivers are located on the free surface and equally spaced at 10 m intervals in the horizontal direction.

First we computed time-domain responses. From time histories we then

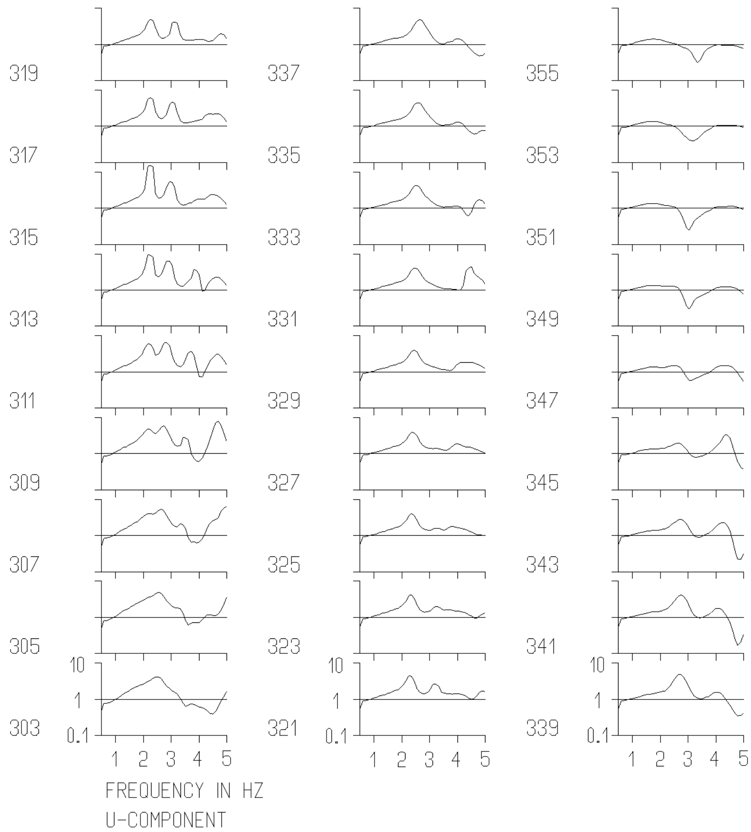

Fig. 3. Amplitude spectral ratios (valley without neighboring ridge/valley with neighboring ridge) for the horizontal component at the receivers on the free surface of the sediment valley. Number 303 denotes the receiver at the left margin of the valley, number 355 denotes the receiver located 15 m to the left of the right valley margin.

computed amplitude Fourier spectra, and, finally, ratios of the amplitude Fourier spectra.

3. Results

Figure 3 shows the spectral ratios for the horizontal component at the receivers on the free surface of the sediment valley. For each receiver the ratio was obtained by dividing the amplitude Fourier spectrum obtained in

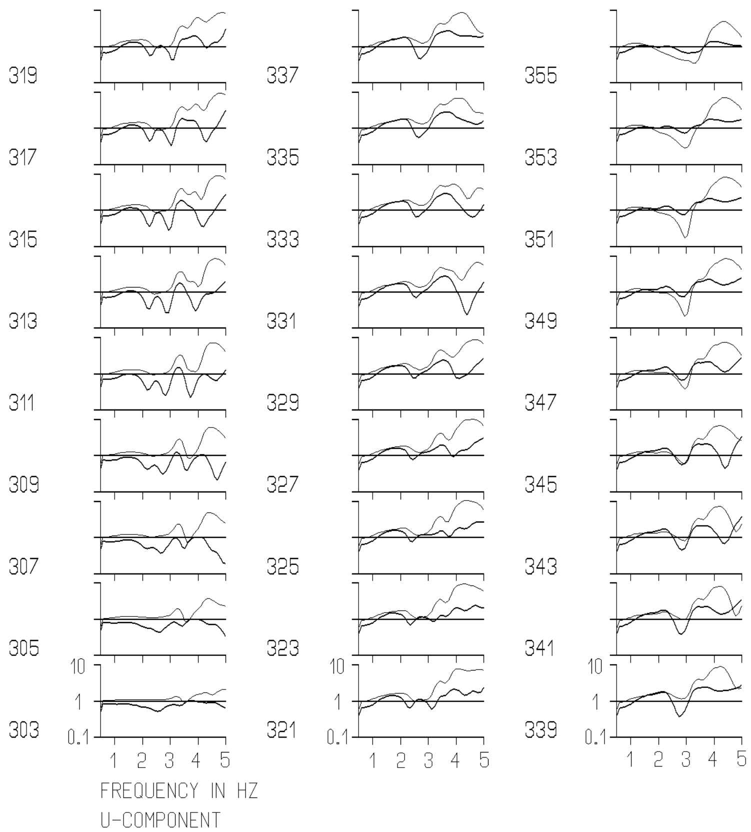

Fig. 4. Amplitude spectral ratios computed with respect to the reference site (receiver No. 297, 30 m to the left of the left valley margin) for the horizontal component at the receivers on the free surface of the sediment valley. Thin line: valley without neighboring ridge; thick line: valley with neighboring ridge.

the case of the valley *without* the neighboring ridge by the amplitude Fourier spectrum obtained in the case of the valley *with* the neighboring ridge. It is clear from the figure that the spectral ratios considerably differ from value of 1 which means that the neighboring ridge has a considerable effect on the valley response. Along a major part of the valley surface the spectral amplitudes are smaller in a presence of the neighboring ridge. We do not show the ratios for the vertical component since those are very close to value of 1. This means that the presence of the neighboring ridge mainly influences the horizontal component in this particular two-dimensional model-wavefield configuration.

The difference between responses of the two valley models can be also seen in the spectral ratios evaluated with respect to a reference site. Figure 4 shows such the ratios for both models. A spectral ratio for a given receiver on the valley surface was computed by dividing the amplitude Fourier spectrum of motion at the receiver by the amplitude Fourier spectrum of motion at the reference site located 30 m to the left of the left valley margin. The spectral ratios evaluated for the valley without the neighboring ridge (thin lines in Fig. 4) considerably differ from those for the valley with the neighboring ridge (thick lines in Fig. 4).

4. Conclusion

A numerical simulation of the seismic response of the sediment valley *with* and *without* neighboring ridge indicates that the valley response may be considerably influenced by the presence of the ridge. This implies that an effect of the neighboring topography should be taken into account in interpretation of the observed earthquake ground motion across the sediment-filled valley.

Acknowledgments. This work was supported in part by Grant No. 205/96/1743, Grant Agency of Czech Republic, and INCO-COPERNICUS Grant PL963311.

References

[1] Aki, K.: Local site effects on ground motion. In: Earthquake Engineering and Soil Dynamics II - Recent Advances in Ground Motion Evaluation, J. L. Von Thun, ed., Geotechnical Special Publication No. *20*, 1988, 103–155, Am. Soc. Civil Eng., New York.

[2] Bard, P.-Y.: Effects of surface geology on ground motion: recent results and remaining issues. In: Proc. of the 10 th ECEE, August 28 - September 2, 1994, Vienna. Balkema, Roterdam, 1995, 305–324.

[3] Bouchon, M., Schultz, C.A. and Toksöz, M.N.: Effect of three-dimensional topography on seismic motion. J. Geophys. Res., *101*, 1996, 5835–5846.

[4] Geli, L., Bard, P.-Y. and Jullien, B.: The effect of topography on earthquake ground motion: A review and new results. Bull. Seism. Soc. Am., *78*, 1988, 42–63.

[5] Moczo, P., Bystrický, E., Kristek, J., Carcione, J.M. and Bouchon, M.: Hybrid modeling of P-SV seismic motion at inhomogeneous viscoelastic topographic structures. Bull. Seism. Soc. Am., *87*, 1997, 1305–1323.